I&EC research
Industrial & Engineering Chemistry Research

Article

pubs.acs.org/IECR

Performance of a Small-Scale Haber Process

Michael Reese,[†] Cory Marquart,[†] Mahdi Malmali,[‡] Kevin Wagner,[‡] Eric Buchanan,[†] Alon McCormick,[‡] and Edward L. Cussler*[,‡]

[†]West Central Research and Outreach Center, 46352 State Highway 329, Morris, Minnesota 56267, United States

[‡]Department of Chemical Engineering and Materials Science, University of Minnesota, 421 Washington Avenue SE # 151, Minneapolis, Minnesota 55455, United States

ABSTRACT: This work identifies a benchmark for the performance of a small-scale ammonia synthesis plant powered by wind energy. The energy used is stranded, far from urban centers but near locations of fertilizer demand. The wind energy drives the pressure swing absorption of air to make nitrogen and the electrolysis of water to make hydrogen. These are combined in the small-scale continuous Haber process to synthesize ammonia. The analysis of runs of the small plant presented in this article permits an assessment of how the current production rate is controlled by three resistances: catalytic reaction, ammonia separation by condensation, and recycling of unreacted gas. The measured catalytic reaction rates are consistent with separate experiments on chemical kinetics and with published reaction mechanisms. The condensation rates predicted are comparable with literature correlations. These rate constants now supply a rigorous strategy for optimizing this scaled-down, distributed ammonia plant. Moreover, this method of analysis is recommended for future small-scale, distributed manufacturing plants.

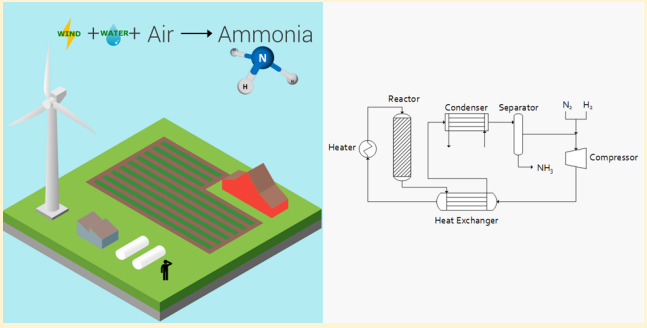

INTRODUCTION

Since the early 1900s, the supply of natural fertilizers has not allowed food production adequate for the growing population. Synthetic ammonia, first developed by Fritz Haber and commercialized by Carl Bosch, has provided the synthetic nitrogen fertilizer required for significant increases in food production around the world.[1,2] After a century of intensive development, this Haber−Bosch process is still the basis for producing more synthetic fertilizer. It is one of the greatest technical innovations known. In addition, in the middle of the 20th century, Norman Borlaug's research improved wheat varieties, resulting in additional food production. This "Green Revolution" required vastly increased amounts of nitrogen fertilizer, with an associated increase in fossil-fuel consumption and carbon emissions.[3] Ammonia is also discussed as an environmentally friendly route to the storage of wind energy.[4,5] Thus, the Haber−Bosch process and the Green Revolution have led to a new challenge for the 21st century: to continue increasing food production while using clean energy, avoiding release of greenhouse gases, and supporting farming for the next generation.[6,7]

We are exploring technologies to make fertilizer using wind power rather than fossil fuels. Such wind-driven ammonia plants will be much smaller than those currently used.[8,9] The plants will use wind to make electricity and then to make ammonia locally. This implies process development in a different direction than that practiced in the traditional chemical industry.[10,11] Such traditional development centers on building bigger plants, which are cheaper because they operate at a larger scale. For processes based on fossil fuels, such larger scales make good sense.

In contrast, in this work, we focus on developing plants that will not be based on fossil fuels drawn from a tanker or a pipeline. Such small plants use renewable wind energy to make small amounts of ammonia for a local market and, so, represent distributed manufacturing, rather than the centralized manufacturing chosen for hydrocarbon feedstocks.[12] We have three objectives in this effort: First, we want to see how the small plant performs as a basis for future technical improvements. Second, we want to explore new ways to separate the ammonia made. Third, we want to study where such small plants should be located. This article is concerned only with the first of these objectives, the small ammonia plant. A companion work will report efforts on new separations and plant location.[13] Together, these works are a first step toward a benchmark for judging how much advantage these small plants can offer.

To see why such an environmentally respectful process might make sense, consider the U.S. wind resources and fertilizer demand shown in Figures 1 and 2, respectively.[14,15] The wind resources in Figure 1 are greater in the more heavily shaded regions of the map. These resources are greatest in regions with low population densities, so the energy they promise is often called "stranded energy": energy that is too far from major

Received: January 5, 2016
Revised: February 27, 2016
Accepted: March 8, 2016
Published: March 8, 2016

DOI: 10.1021/acs.iecr.5b04909
Ind. Eng. Chem. Res. 2016, 55, 3742−3750

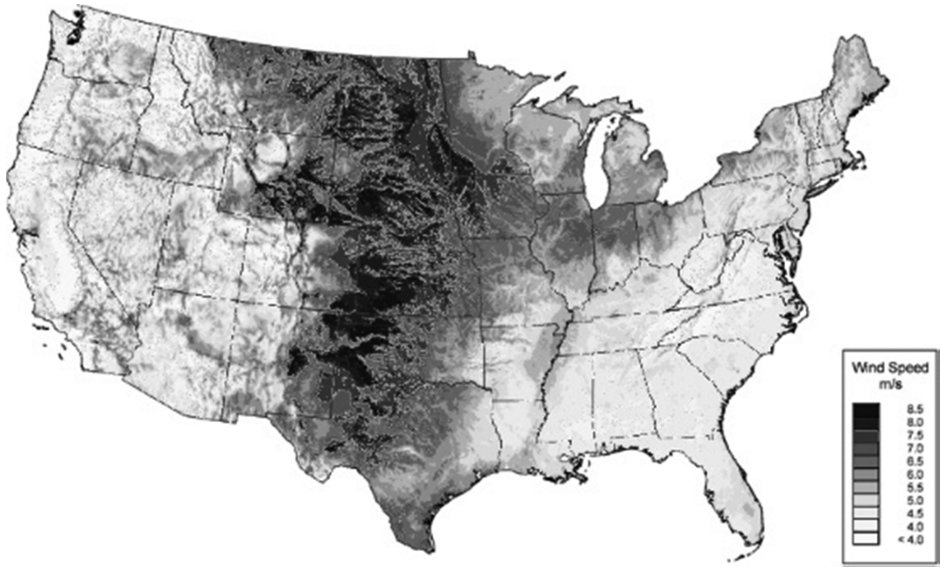

Figure 1. Wind resources in the United States. The greatest potential sources of wind power, which are darker in the figure, are in areas with small populations. As such, they represent so-called stranded energy that can be used to make ammonia. (Figure adapted from ref 14.)

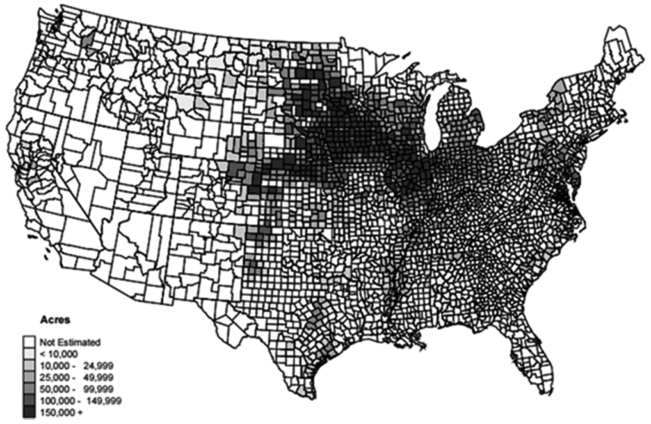

Figure 2. Ammonia demand in the United States. The regions of greatest ammonia demand, shown as the darker areas, roughly coincide with the areas of greatest potential wind energy. (Figure adapted from ref 15.)

population centers to be used without excessive losses in transmission. At the same time, the fertilizer demand, that is, where ammonia is most needed (see Figure 2), is in roughly the same regions of the country as the stranded energy. This is one reason why projects converting wind to ammonia might make sense: The energy is there, but it will not be used directly by concentrated populations for electricity.

We have already demonstrated the promise of farm-scale, wind-based, environmentally benign ammonia synthesis in a unique facility, namely, the Renewable Hydrogen and Ammonia Pilot Plant, the first local farm-to-coop scale system for fertilizer production. An analysis of the first technical data from this facility, dedicated in summer 2013 at the West Central Research and Outreach Center (WCROC) in Morris, MN, is reported here. It is a scaled-down version of the conventional ammonia synthesis process; however, rather than using fossil fuels, it uses wind energy.

In other respects, this small-scale process is conventional, as shown schematically in Figure 3. Hydrogen and nitrogen enter the process in the upper right-hand corner, are combined with

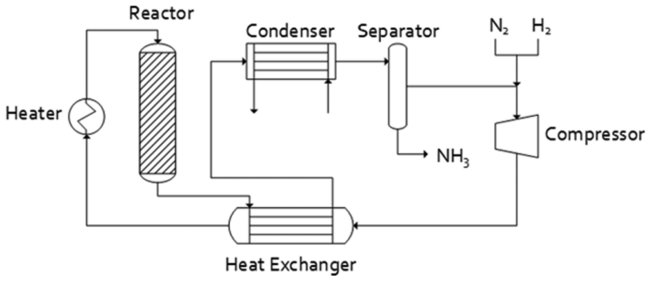

Figure 3. Schematic drawing of the Haber process small-scale plant. Hydrogen and nitrogen fed to the plant are mixed with recycled gases and compressed. They are preheated using gases exiting the reactor and then pass over the catalyst in the reactor. Then, the ammonia in this effluent is condensed and harvested.

recycled gases, and are fed to a compressor. The resulting gas mixture flows through one side of a heat exchanger to a heater and then into the reactor. The reaction, catalyzed by a conventional ammonia synthesis catalyst, increases the amount of ammonia in the exiting gas mixture, which is cooled when it flows through the other side of the heat exchanger. The gas mixture is then further cooled to condense liquid ammonia, which is removed in the separator. Gases that are not condensed are returned to the compressor.

In the remainder of this article, we report a model and data for this process to investigate whether they are consistent with the optimal production rates. We then discuss how these results can guide our search for optimized small-scale, distributed ammonia production.

THEORY

To guide our analysis of the results found from the small plant, we derive an approximate model based on the schematic drawing shown in Figure 3. In this derivation, we assume that the process is at steady state and that the reactor and condenser gases are well-mixed, so that the concentrations exiting these regions are the same as those present in these regions.[16,17] This implies that the average nitrogen concentration in the reactor equals the nitrogen concentration at the exit. Although this is

DOI: 10.1021/acs.iecr.5b04909
Ind. Eng. Chem. Res. 2016, 55, 3742−3750

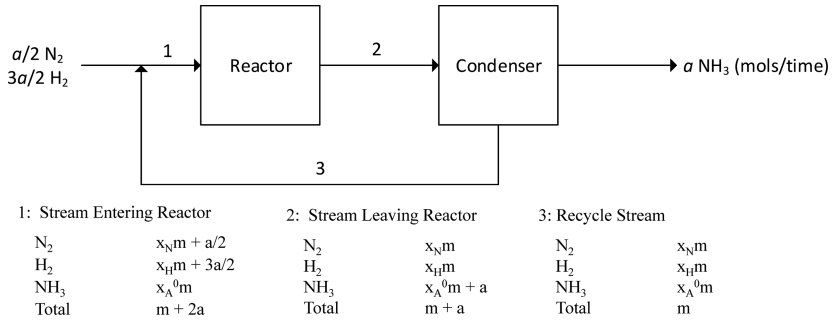

Figure 4. Simplified block diagram of the small plant. The contents of the reactor and condenser are assumed to be well-mixed, as justified in the text.

certainly untrue if most of the nitrogen entering the reactor reacts in a single pass, it is much more nearly true when little reacts in a single pass, so that the amount recycled is large relative to the amount reacting. As we will show, this is the case for this plant.

To put these ideas on a more quantitative basis, we define a as the number of moles per unit time of liquid ammonia removed from the condenser and m as the molar flow rate of gas mixture exiting the separator. The recycle stream then has $x_A m$ moles of ammonia per unit time, $x_H m$ moles of hydrogen per unit time, and $x_N m$ moles of nitrogen per unit time, where x_i represents the mole fraction of component i in the recycle stream. The stream entering the reactor has $x_A m$ moles of ammonia per unit time, $x_H m + 3a/2$ moles of hydrogen per unit time, and $x_N m + a/2$ moles of nitrogen per unit time; the stream leaving the reactor contains $x_A m + a$ moles of ammonia per unit time, $x_H m$ moles of hydrogen per unit time, and $x_N m$ moles of nitrogen per unit time. Figure 4 presents a simplified block diagram of the small-scale ammonia synthesis plant.

We next supplement these mass balances with rate equations for the reactor and the condenser. For the chemical kinetics in the reactor, the rate expression for the balance on ammonia is

$$0 = -a + k_R V_R \left[x_A^* - \left(\frac{x_A^0 m + a}{m + a} \right) \right] \tag{1}$$

where k_R is the linearized apparent catalytic reaction rate constant, V_R is the volume of catalyst, x_A^* is the ammonia mole fraction at equilibrium, and the quantity in parentheses is the ammonia mole fraction actually in the reactor. If x_A^* equals this actual mole fraction, the reaction is at equilibrium. The details of the linearization and of finding the numerical values of the rate constant are shown in the Results section below.

This equation is a major approximation, not only because of the assumption of good mixing in the reactor. It also implicitly assumes that the reaction is first-order. However, this is not true: For example, in the widely quoted Temkin–Pyzhev equation,[18−21] the forward rate of reaction depends nonlinearly on the partial pressures of ammonia, nitrogen, and hydrogen. Here, by approximating this rate as a single quantity (i.e., $k_R V_R$) with dimensions of moles per unit time, we acknowledge that this rate constant will vary not only with temperature and catalyst volume, but also with mole fractions in the reactor and with the reactor pressure.

The second balance, on the condenser, is also at steady state

$$0 = a - k_c A_c (x_A - x_A^0) \tag{2}$$

where k_c is the mass-transfer coefficient between the bulk vapor; x_A is the ammonia mole fraction; x_A^0 is the equilibrium mole fraction at the cold condenser wall, equal to the saturation vapor pressure divided by the total pressure; and A_c is the condenser's interfacial area. Like $k_R V_R$, the quantity $k_c A_c$ has dimensions of moles per unit time; unlike $k_R V_R$, however, it depends only weakly on temperature and more strongly on physical factors such as flow and surface geometry. The approximation of mass transfer as a first-order process is much less severe than the corresponding approximation of reaction kinetics. Nevertheless, k_c might be a weak function of $x_A - x_A^0$ because of free convection.

We now combine eqs 1 and 2 to find the ammonia production a in terms of the known concentrations x_A^* and x_A^0, which are known at the temperature and pressure of the reactor and condenser, respectively. From eq 2

$$x_A = x_A^0 + \frac{a}{k_c A_c} \tag{3}$$

The concentration in the recycle, x_A, is always larger than that found from the saturation vapor pressure x_A^0. From eq 1, we write

$$a = \frac{b}{2}\left(\sqrt{1 + \frac{4c}{b^2}} - 1 \right) \tag{4}$$

where

$$b = m k_R V_R \left(\frac{1}{k_R V_R} + \frac{1}{k_c A_c} + \frac{1 - x_A^*}{m} \right) \tag{5}$$

and

$$c = m k_R V_R (x_A^* - x_A^0) \tag{6}$$

This is the key result of the model.

The physical meaning of this result can be clarified if one recognizes that the term $1/k_R V_R$ is the resistance due to the chemical reaction. Similarly, $1/k_c A_c$ and $(1 - x_A^*)/m$ are the resistances of the condenser and of the recycle loop, respectively. Moreover, the ratio c/b^2 in eq 4 can be rearranged as

$$\frac{c}{b^2} = \left[\frac{(x_A^* - x_A^0)/m}{\frac{1}{k_R V_R} + \frac{1}{k_c A_c} + \frac{1 - x_A^*}{m}} \right] \left(\frac{\frac{1}{k_R V_R}}{\frac{1}{k_R V_R} + \frac{1}{k_c A_c} + \frac{1 - x_A^*}{m}} \right) \tag{7}$$

The numerator of the first term in brackets on the right-hand side of eq 7 is the driving force for the reaction. As long as the ammonia concentration in the inlet stream to the reactor (x_A^0)

DOI: 10.1021/acs.iecr.5b04909
Ind. Eng. Chem. Res. 2016, 55, 3742−3750

is less than the ammonia saturation mole fraction at the reactor pressure and temperature (x_A^*), the production of ammonia takes place. The denominator of the first term in brackets on the right-hand side is the total resistance normalized by the recycle, and the term in parentheses on the right-hand side of eq 7 is the fraction of the total resistance due to the reaction.

To see how these different factors affect ammonia production, it is helpful to examine the result of a Taylor series expansion of the square root in eq 4, which gives

$$a = \frac{x_A^* - x_A^0}{\frac{1}{k_R V_R} + \frac{1}{k_c A_c} + \frac{1 - x_A^*}{m}} \tag{8}$$

This behavior is observed in many rate processes with recycle and separation: The amount produced is proportional to the overall driving force divided by the total resistance.[17] The total resistance is the sum of the resistances of reaction, condensation, and recycle. Phrased in other terms, it is a weighted harmonic average of the speeds of these three steps, so that the lowest speed has the greatest effect on the rate of ammonia production. If the reactor is undersized or operating at a temperature that is too low, the reactor resistance will dominate. If the condenser is undersized, the condenser resistance will dominate, and if the recycle rate is too low to take full advantage of the unit operations, the recycle resistance will dominate. We use this model and these results to analyze the experimental plant runs described next and, hence, to explore how this small-scale plant can be made more productive. In pursuing this case study, we recommend this procedure for the analysis of other such small-scale, distributed processes.

EXPERIMENTAL SECTION

Plant Details. The ammonia synthesis plant that is the key to these experiments is shown schematically in Figure 3. The entire system is powered by electricity either produced by a 1.65 MW wind turbine (Vestas, Aarhus, Denmark) or from the local utility (Ottertail Power Company, Fergus Falls, MN). Nitrogen is produced by an Innovative Gas Systems NS-10 pressure swing adsorption system (Grosseto, Italy). The nitrogen it produces, which is greater than 99.9% pure, is stored at ambient temperature at a pressure of 165 bar in 18 tanks, each with a volume of 0.05 m^3 (Norris Cylinder Company, Longview, TX). Hydrogen, which is generated by a Proton Onsite Hogen H6 system (Wallingford, CT), is over 99.9% pure after being dried across phosphorus pentoxide. It is stored at ambient temperature and 165 bar pressure in 54 0.05 m^3 tanks identical to those used for nitrogen. Both of these systems function properly; occasionally, the hydrogen production was marginally less than the amount required for the synthesis.

The nitrogen and hydrogen gases flow through an orifice meter (Imperial Flange & Fitting Company Inc., Los Angeles, CA) into the main system, where they are combined with recycled gases coming from the separator. These mixed gases, at 83 bar, enter an RIX Industries (Benicia, CA) 4VX1BG-1.7 compressor. The exiting gases leave at a pressure of about 145 bar and flow to a train of four double-pipe heat exchangers, where they are warmed using the gases that are discharged from the reactor. The inner pipe of each heat exchanger (Sep-Pro Systems Inc., Houston, TX) has an inside diameter of 0.013 m and a length of 20.3 m, giving a total interfacial area of 0.83 m^2. These gases, now at a pressure of about 145 bar, flow to a 20 kW heater (Sep-Pro Systems Inc., Houston, TX), where they can be heated to reactor temperature.

The hot gases then flow to the reactor (Consolidated Inc., Gary, IN), which is 2.23 m long and 0.203 m in diameter and is sealed with a metal O-ring made of stainless steel. Tightening this O-ring to avoid leaks requires considerable care using hydraulic torqueing of the bolts that secure the top flange to the reactor body. Within the reactor, the catalyst is contained in an annular basket (Consolidated Inc., Gary, IN) that is 1.8 m long and has a 0.152-m outer diameter. To load the catalyst, the top flange is removed, and the catalyst is poured into the basket. The reagent gas feeds into the lumen of this annular space and flows radially out through the catalyst. The particular catalyst used is AmoMax-10 (Sud-Chemie, Louisville, KY). The gases exiting the reactor flow back through the shell side of the heat exchanger and, so, preheat the reactive feed.

These gases now flow to the condenser (Sep-Pro Systems Inc., Houston, TX), which has one tube that is 8.4 m long and 0.013 m in diameter, giving a condenser surface area of about 0.34 m^2. A refrigeration skid (Sep-Pro Systems Inc., Houston, TX) drives the refrigerant, R-404A (Copeland, Sidney, OH), through an 8.4-m-long, 0.025-m-diameter outer shell around the condenser tube. It operates at about −20 °C. The resulting gases exit from the condenser at a temperature of about −17 °C and flow to the separator, a flash drum. The flash drum separates the ammonia liquid. Ammonia separated in the flash drum exits the plant through a solenoid valve and flows to a larger storage tank. The ammonia collected is stored in an 11.7 m^3 storage tank (WestMor Industries, Morris, MN) at a pressure of 10 bar. The uncondensed gases are mixed with the incoming feed and recycled back into the compressor to start the process again.

The piping used for this plant, most of which was purchased from Swagelok (Chaska, MN), is made from two different materials: carbon steel and stainless steel. Embrittlement with hydrogen is always a problem. All tubing is fixed inside the pilot skid. Unless the tubing is stressed, the risk of leaking is very small. However, the corrosive nature of ammonia worsens the situation. Typically, in the tubing through which the hot gas mixture is transported between heat exchanger and reactor, stainless steel 316L is employed because it is more resistant toward corrosion by hot ammonia. In the tubing through which the low-temperature gas mixture is transported among the heat exchanger, separator, and compressor, carbon steel is used. Carbon steel has a higher resistance toward high pressure and a longer lifetime in the presence of hydrogen.

The chief difficulties in startup were plumbing of the vent ports on the mixed-gas compressor and leaks throughout the skid. Holes on the side and bottom of the reactor, which had been drilled for testing, also leaked and, so, were welded shut with a certified R-stamp welder. Some of the equipment also had material that was not compatible with ammonia and had to be replaced or repaired. Significant effort was required to understand and program the control systems.

Now that the small plant is capable of producing extended runs at steady state, we are able to subject its performance to the analysis described in the Theory section.

Laboratory Kinetic Experiments. To estimate the reactor resistance, we needed to test the catalyst used in the small plant. This was accomplished using a laboratory-scale reactor with the same catalyst. The reactant gases N_2 and H_2, of ultrahigh purity, were purchased from Matheson (New

DOI: 10.1021/acs.iecr.5b04909
Ind. Eng. Chem. Res. 2016, 55, 3742−3750

Brighton, MN). The stainless steel reactor was tubular, 0.38 m long and 6.4 mm in diameter. The first and last 0.13-m sections of the reactor were filled with stainless steel wool, and the catalyst was packed in the middle. The catalyst, the same as in the small plant, with a nominal size range of 1.5−3 mm, is also stabilized with an oxygen-rich protective layer. The reactor used an Omega ceramic heater (CRFC-36/115-A, Stamford, CT) equipped with an Omega multiramp proportional−integral−derivative (PID) controller (CN96211TR) to control the temperature. The inlet and outlet gas temperatures and the reactor surface temperature were measured using K-type thermocouples connected to an Omega signal conditioner (DRG-SC-TC). The system pressure was recorded using a WIKA pressure transducer (50426877, Lawrenceville, GA) with 0−10 V dc output.

The experiments were carried out in circulation batch with a variable piston pump (model PW2070N, PumpWorks, Minneapolis, MN). Data were recorded every second using a National Instruments LabVIEW program that also controlled the mass flow controllers, which injected known volumetric flows of reactant gases into the reactor. Before each run, the system was tested for leaks for 3 h, using nitrogen at 1500 psi. To remove the oxidized protective layer and activate the catalyst, the system was pressurized at 200 psi with 500 cm^3 (STP)/min hydrogen. The temperature was slowly raised for 27 h to reach to 723 K. The hydrogen flowed through the catalyst bed for at least 24 h at this temperature. After activation, the system was kept under nitrogen.

RESULTS

Our analysis centers on five runs carried out in the small-scale plant for times ranging from 4 to 43 days. The runs had reactor exit temperatures of about 565 K and pressures of about 115 bar. More specific parameters are given in Table 1. Although

Table 1. Basic Data for Five Process Runs[a]

start date	T^b (K)	P^b (bar)	run (days)	N_2 feed (mol/h)
07/14/2014	569	112	4	63
09/02/2014	575	72	4	62
09/07/2014	563	124	30	41
10/29/2014	**565**	**117**	**33**	**47**
01/09/2015	557	128	43	35

[a]Values are averages for the entire run. [b]Measured at the reactor exit.

the runs differed slightly, they produced similar results; for illustration, we discuss in detail only the run begun on October 29, 2014 (highlighted in bold in Table 1), judging it to be typical.

The temperature and the recycle obtained for the run of 10/29/2014 are shown in Figure 5. During the first 3 days, there were excursions not only in temperature and pressure but also in recycle rate. Additionally, we observed a small spike in pressure on days 18−21, mainly due to the difficulty associated with controlling the operation of the small plant. As a result, we discarded the data obtained on days 1−3 and 18−21 and concentrated our analysis on two divided periods on days 4−18 and days 21−33.

The data in Figure 5 show that the small plant is operating near steady state. The pressure is almost constant, varying by less than 5%. The recycle rate is also nearly constant, fluctuating by 7%. The temperature shows greater excursions, by as much as 50 °C. These excursions seem to be uncorrelated with the

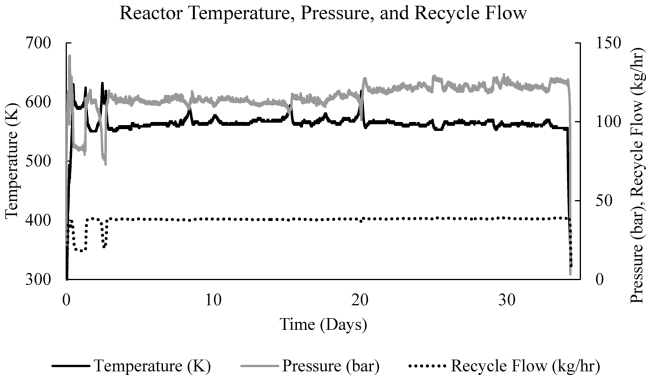

Figure 5. Reactor temperature and pressure in an example plant run. After the transients in the first 3 days, the plant process operates near steady state. The recycle flow is also constant in time.

pressure and the recycle flow. Such a lack of correlation might reflect control of the synthesis by chemical reaction, as explored in the Discussion section below.

The feeds of nitrogen and hydrogen are in a ratio of 3:1, the ratio consistent with the reaction's stoichiometry. Although these data show steady operation over days, the feeds are subject to considerable variation over hours, as shown in Figure 6. The fluctuations in nitrogen flow rate, which are smaller,

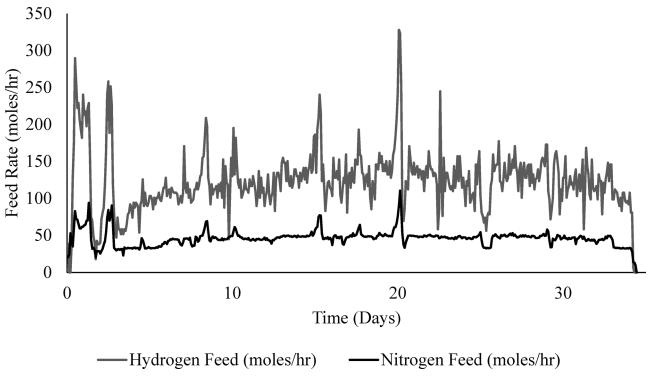

Figure 6. Nitrogen and hydrogen flows into the plant in an example plant run. These flows, averaged over time, are in the stoichiometric ratio of 3:1.

might be caused by changes in the pressure swing adsorption unit, which are not completely damped out by the storage tank for nitrogen. The larger fluctuations in hydrogen are due primarily to the operation of the electrolysis unit. Occasionally, the electrolysis unit appeared not to supply hydrogen at the rate needed by the small plant. When this happened, we reduced the nitrogen flow rate. Still, even with these occasional variations, the temperature, pressure, and recycle rate remained relatively constant, as shown by the data in Figure 5.

We now turn to the implications of the data in Figures 5 and 6 using the model developed in the Theory section. These are shown in Table 2 for the earlier and later periods of the experiment begun on 10/29/2014. The second column in Table 2 includes the average feed rates of nitrogen and hydrogen. There is no ammonia in this fresh feed. The third, fourth, and fifth columns in the table give the flows at different points within the process. These internal flows are greater than the amounts of nitrogen and hydrogen actually fed, as is characteristic of most ammonia synthesis plants. To get fast kinetics, the reactor temperature and pressure should be high.

DOI: 10.1021/acs.iecr.5b04909
Ind. Eng. Chem. Res. 2016, 55, 3742−3750

Table 2. Gas Flows (mol/h) within the Steady-State System (10/29/2014 Run[a])[b]

	new feed	flow into reactor	flow out of reactor	flow out of condenser	product
			Day 4–Day 18		
N_2	40 (0.22)	1100 (0.25)	1000 (0.23)	1000 (0.24)	0
H_2	140 (0.78)	3100 (0.70)	3000 (0.70)	3000 (0.71)	0
NH_3	0	230 (0.05)	320 (0.07)	230 (0.05)	90
total	~180	~4400	~4300	~4200	
			Day 21–Day 33		
N_2	47 (0.25)	1100 (0.24)	1100 (0.24)	1100 (0.24)	0
H_2	140 (0.75)	3400 (0.74)	3300 (0.72)	3300 (0.74)	0
NH_3	0	64 (0.02)	160 (0.04)	64 (0.01)	90
total	~190	~4600	~4600	~4500	

[a]Average temperature, 565 K; average pressure, 113 bar. [b]Values in parentheses are mole fractions.

However, the high temperature producing the fast kinetics also means the conversion at equilibrium is limited. This means that large amounts of unreacted gases must be separated from the ammonia produced, which, in this case, is removed by condensation. In addition to the unreacted hydrogen and nitrogen, there will also be a substantial amount of ammonia that is not removed in the condenser. As a result, the total recycle stream here is about 20 times the new feed stream, as values in the Table 2 show. This is true in both the experiments during days 4–18 and the experiments during days 21–33.

Regrettably, the plant does not currently contain the instrumentation to measure these flows more directly. Although the orifice meters measuring the nitrogen and hydrogen flows are operating at Reynolds numbers of about 5000, where calibration is difficult, we believe that the orifice measurements are reliable. The flow of the recycled gases is 70% of the maximum flow possible in this pump, consistent with the design.

In the future, we plan to modify the equipment to allow higher temperatures, to ensure that the nitrogen and hydrogen flows are accurate, and to measure the concentrations in the recycle stream. Part of the point of the analysis in this article is to check our intuition that (a) the current production rate is limited by the reaction and (b) the other components of the system will be able to accommodate increased production if the reaction rate is increased.

Finally, before we discuss these results, we need to report our laboratory measurements of ammonia kinetics compared with those predicted from literature sources, summarized as the Temkin–Pyzhev equation. This comparison is given in Figure 7, where our measurements at the temperatures and pressures shown are compared with those expected from other references.[19−22] The figure shows that the agreement is good (R^2 = 0.98). We use these values in the estimates of the different resistances to ammonia synthesis in the discussion of the small-plant performance that follows.

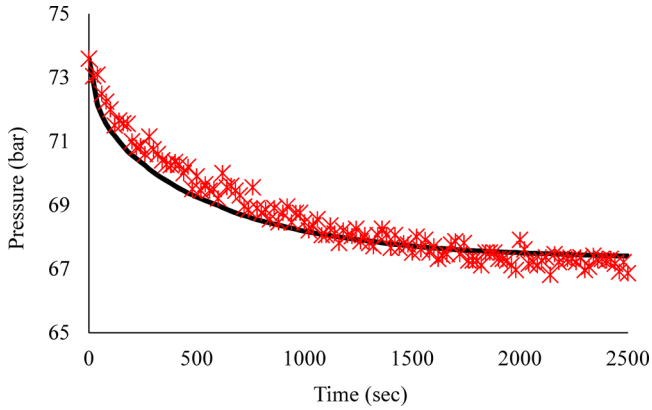

Figure 7. Laboratory-measured vs literature-calculated reaction kinetics at 723 K. The rates measured from laboratory kinetic experiments (shown by markers) in this work agree with those estimated from the literature[19−22] (solid line).

DISCUSSION

The results reported in the preceding section show that the small plant works and can produce extended runs of data logging at steady state. It makes ammonia with wind energy. It does so with nitrogen made by the pressure swing adsorption of air and with hydrogen from the electrolysis of water. The pressures used are near those specified in the design, although the reactor temperature is about 100 K less than the temperature of a conventional reactor as originally sought.

Still, these early results supply a template on how to proceed. They should allow the costs for small-scale ammonia synthesis to be detailed. Indeed, we have already made an early economic analysis of these data.[11] We have used these results to start to identify where small plants for distributed ammonia production should be located.[13]

Nonetheless, the core of this article is the exploration of the technical limitations and opportunities for this small-scale technology. We have a sound start, but there is a shortfall in the intended ammonia production. We assume that this is probably the result of the limited temperature achieved in the reactor. We reached a temperature of about 565 K, whereas the design target was 670 K. Had we been able to achieve this higher temperature, we might expect a corresponding increase in ammonia production—as long as the separator and the recycle can keep up with the increased production. We discuss this exploration with some rigor next.

Our immediate efforts to extend this technology combine these preliminary experiments with the analysis suggested by the model developed in the Theory section. This model, summarized in eq 4 or 8, predicts that the ammonia synthesis by the entire process is proportional to an overall rate constant times an overall driving force. The overall rate constant is a harmonic average of the three rate constants of the reaction, the ammonia separation, and the recycle. The overall driving force is the ammonia concentration that would exist at equilibrium, x_A^*, minus the ammonia concentration in the vapor in the condenser, x_A^0.

The values of the three rate constants merit careful consideration, as they are the key by which the process will be improved. For instance, it would not make sense to take

DOI: 10.1021/acs.iecr.5b04909
Ind. Eng. Chem. Res. 2016, 55, 3742−3750

measures to increase the reactor temperature if we found that the overall production rate is limited by the separator capacity. In each case, we linearize the rate constants for small deviations from equilibrium.

Linearized Rate Constant for Reaction. The rate constant for the reaction is the most complex. This reaction rate is most often correlated using the Temkin−Pyzhev equation[18−21]

$$r = k_1 \frac{p_{N_2} p_{H_2}^{1.5}}{p_A} - k_2 \frac{p_A}{p_{H_2}^{1.5}} \tag{9}$$

This equation can be rewritten by defining the variable

$$X = \frac{P_A^* - P_A}{P_{N_2}^*} \tag{10}$$

and for stoichiometric feed with no purge

$$\frac{X}{2} = \frac{P_{N_2} - P_{N_2}^*}{P_{N_2}^*} = \frac{P_{H_2} - P_{H_2}^*}{P_{H_2}^*} \tag{11}$$

Linearization using the Taylor series for small values of X simplifies this substitution to yield

$$r = k_1 \frac{P_{N_2}^* P_{H_2}^{1.5*}}{P_A^*}\left(1 + \frac{5}{4} + \frac{P_{N_2}^*}{P_A^*}\right)X - k_2 \frac{P_A^*}{P_{H_2}^{1.5*}}\left(1 - \frac{P_{N_2}^*}{P_A^*} - \frac{3}{4}\right)X \tag{12}$$

Subtracting the concentrations at equilibrium gives

$$r = k_1 \frac{P_{N_2}^* P_{H_2}^{1.5*}}{P_A^*}\left(\frac{9}{4} + \frac{P_{N_2}^*}{P_A^*}\right)(X - X^*) + k_2 \frac{P_A^*}{P_{H_2}^{1.5*}}\left(\frac{P_{N_2}^*}{P_A^*} - \frac{1}{4}\right)$$
$$(X - X^*) = k_R'(X - X^*) \tag{13}$$

where k_R' is a linearized overall rate constant with dimensions of moles of ammonia per catalyst volume per time, which is different from k_R in eq 1 by a factor of 4. We used two different approaches to calculate this linearized reaction rate constant for the plant reactor's temperature. The first approach was to calculate the linearized rate constant for each temperature, plot the logarithms of these constants versus the reciprocal of temperature, and use the data to extrapolate to find the rate constant of the plant process at 565 K. The resulting Arrhenius plot is shown in Figure 8. This first approach gives a value for k_R of 0.67 mol/L·h. Because the catalyst volume is 12 L, the characteristic rate constant, $k_R V_R$, is 14 mol/h. The second approach was to plot the Arrhenius equation for k_1 and k_2 and extrapolate to find the values at the plant temperature. Then, we used the extrapolated values to calculate k_1 and k_2 at 565 K and substituted these values into eq 13 to determine the linearized k_R. Although this approach gave a value of 0.23 mol/L·h, smaller than that of the first method, the fit of the plots was poorer. As a result, we used the first approach to calculate the values used in our analysis. Finally, the small-plant system contains n_0 = 113 mol of gas mixture actually present in the system. Thus, the characteristic time for the reaction is 14 h.

Characteristic Rate Constant for Condensation. We next turn to the second rate constant of the small-plant process, that associated with the condenser. The condensation rate is

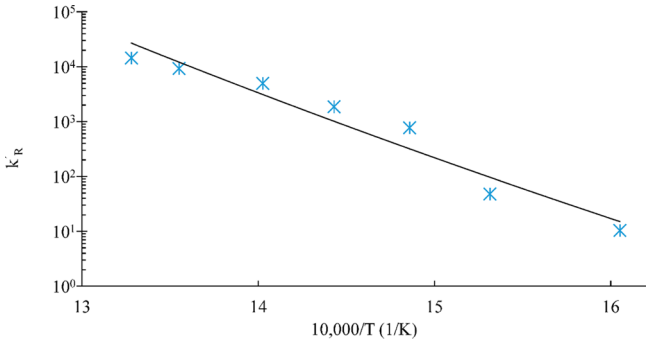

Figure 8. Linearized reaction rate vs temperature. The reaction rate values, obtained from laboratory kinetic experiments, extrapolated to the plant reactor temperature of 565 K, were used in estimating the characteristic times in Table 3.

affected both by the rate of mass transfer on the reactive gas side and by the heat transfer on the refrigerant side. At present, we have no basis for determining which of these rates is more important. From the Chilton−Colburn analogy,[22] we suspect that they will be similar in magnitude. As a result, we decided to make our first estimates based on heat transfer, because the correlations are better developed.

Our estimate of this rate, then, begins with the overall heat-transfer coefficient U

$$1/U = 1/h_o + 1/h_w + 1/h_j \tag{14}$$

where U and h_j are overall and individual heat-transfer coefficients, respectively, and the subscript j refers to the external (o), wall (w), and internal (j) surfaces. The gas stream entering the condenser is expected to be at 333 K (recorded from the plant temperature indicator), with a mass flow rate of 38 kg/h.[23] In the condenser, this flow is cooled on the shell side with R-404A refrigerant, which is expected to have an external heat-transfer coefficient h_o of about 2000 W/m^2·K.[24] Because the condenser tubes are constructed of 4-mm-thick carbon steel (SA-333-6), the wall heat-transfer coefficient is over 50000 W/m^2·K. The piping for the condenser is a 12.7-mm schedule 80 pipe, with a wall thickness equal to about 4 mm. The heat-transfer coefficient for ammonia condensing inside the tube is about 4000 W/m^2·K. Thus, the overall heat-transfer coefficient is equal to 1300 W/m^2·K. Previous literature supports this estimate for ammonia condensation.[25] Because the condenser wall is at the refrigerant temperature (250 K), the heat of vaporization of ammonia is 22.8 kJ/mol, and the total area for heat transfer is 0.343 m^2, the rate constant for evaporation is

$$k_c A = \frac{UA\Delta T}{\Delta H_{vap}} = \frac{1300 \times 0.343 \times [333 - (250)] \times 3600}{22.8 \times 10^3}$$
$$= 5850 \text{ mol/h} \tag{15}$$

Again, the apparatus contains 113 mol of gas mixture, so the characteristic time for the condenser is 0.020 h. This is much shorter than the reaction time.

Characteristic Rate Constant for Recycle. The third rate constant that affects the process is that associated with the recycle pump. The equilibrium mole fraction at the operating pressure and temperature of 565 K and 117 bar, respectively, is 0.58. Because the data show recycle flow rates of about 4400 mol/h, the pumping characteristic time for the 10/29/2014 run is defined as

DOI: 10.1021/acs.iecr.5b04909
Ind. Eng. Chem. Res. 2016, 55, 3742−3750

Table 3. Characteristic Process Properties for a Stoichiometric Ratio of Nitrogen to Hydrogen of 1:3

	07/14/2014	09/02/2014	09/17/2014	**10/29/2014**	01/09/2015
T (K)	569	575	563	**565**	557
p (bar)	112	72	124	**117**	128
m (mol/h)	3300	2200	4400	**4400**	4400
n_0 (mol)	110	68	120	**110**	120
x_A^*	0.56	0.53	0.58	**0.55**	0.60
x_A^0	0.033	0.047	0.019	**0.016**	0.013
condenser T (K)	400	360	420	**410**	420
$n_0/k_R V_R$ (h)	2.4	0.92	4.5	**3.5**	7.5
$n_0/k_c A_c$ (h)	0.019	0.012	0.021	**0.020**	0.022
$n_0(1 - x_A^*)/m$ (h)	0.014	0.015	0.011	**0.011**	0.011

$$\text{pumping time} = \frac{n_0(1 - x_A^*)}{m} = \frac{113(1 - 0.58)}{4400} = 0.011 \text{ h} \quad (16)$$

This is smaller than both the reaction time and the heat-transfer time.

Comparing Characteristic Rate Constants As Characteristic Time Constants. To explore the meaning of these times more completely, we turn to the summary of results in Table 3. This table shows more complete data for the five runs mentioned in Table 1, identified with the dates in the column headings. The results for the experiment started on 10/29/2014 are those detailed above and shown in bold. However, all five experiments give similar results. Rows 1 and 2 in the table give the temperature and pressure of the experiments. Rows 3 and 4 give the moles per hour recycled in the process (m) and the total number of moles actually present in the reactor, n_0, respectively. Rows 5 and 6 give the mole fractions at equilibrium of ammonia in the reactor and in the condenser, respectively; the difference between these values is the overall driving force for the process, as summarized in eq 8. Row 7 gives the temperature in the condenser. Most importantly, rows 8−10 give the times for the three rates of reaction, condensation, and recycle, respectively. We use the total number of moles of gas in the plant to fashion these as characteristic times. The longest time, which corresponds to the slowest step, controls the overall rate of the process; this is the characteristic time associated with the principal resistance to the overall plant production rate.

Under the process conditions used so far, the unit operation dominating the rate of production is the reactor. Upon reflection, this is not surprising. A review of the operating logs shows that the reactor operating temperatures used in the runs to date have been substantially below those characteristic of the use of this catalyst in conventional plants (ca. 700 K). We also see that the other two characteristic times, of the condenser and of the recycle, are 3 orders of magnitude smaller: These units are quite capable of handling increased production rates. If the reaction temperature could be increased to 700 K, the characteristic time of the reaction rate constant would equal that estimated for the condenser, and the plant performance would be closer to optimal. This optimum might be found at lower temperatures if, as expected, the condenser time includes resistance to mass transfer in the ammonia, as well as heat-transfer resistance in the refrigerant; only the latter contribution has been considered so far.

In this case study, our analysis suggests that the recycle and separation capacities of the current small plant are more than adequate to accommodate increased reactor performance. However, we note that the separation or recycle capacity might well be judged limiting in other cases, and these operations are felt to influence broad sections of the chemical industry.[17]

This simple method of analysis, we suggest, should be useful for many current efforts to produce small-scale, distributed manufacturing processes. We note that the principles guiding downscaling are not as familiar as those for upscaling, in large part because the economic driving forces can be unusual (e.g., stranded power, zero-carbon incentives) and also in part because the capital cost is often governed by custom manufacturing. Thus, it is useful to analyze prototype small plants to optimize operation.

■ CONCLUSIONS

In this work, we have presented a benchmark for the performance of a small-scale ammonia synthesis with a zero-carbon footprint. Stranded wind energy supplies the energy for this process, and the feed is provided from renewable resources. Such a process can satisfy fertilizer demand in distant locations with limited access to conventional energy resources. Generally, controlling small-scale processes is difficult, and this process is not operating under its best conditions. To further understand the ammonia synthesis in our small-scale Haber−Bosch plant and determine the optimal conditions for operation, we simplified the ammonia production process to three main steps operating in series: reaction, separation, and recycle. This simplified model successfully predicts the performance of different units and gives information regarding each region.

Our laboratory-scale kinetic studies along with our linearized reaction rate show that the chemical reaction is rate-limiting. Our analysis indicates that the catalytic reaction resistance of the currently operating plant is at least 3 orders of magnitude larger than the condensation and recycle resistances. Our kinetic studies support the suggestion that increasing the reaction temperature to approximately 700 K would lead to a reaction resistance of the same order of magnitude as the condensation resistance. In this instance, we have shown that there is no reason to be concerned that the increased production rate might not be accommodated by the separator or the recycle capacities. Such a straightforward model might help to explain the design of other small-scale processes in the future.

■ AUTHOR INFORMATION

Corresponding Author

*Tel.: 612-625-1596. Fax: 612-626-7246. E-mail: cussler@umn.edu.

DOI: 10.1021/acs.iecr.5b04909
Ind. Eng. Chem. Res. 2016, 55, 3742−3750

Notes

The authors declare no competing financial interest.

■ ACKNOWLEDGMENTS

This work was primarily supported by MNDrive, an initiative of the University of Minnesota; and by the Minnesota Environment and Natural Resources Trust Fund as recommended by the Legislative-Citizen Commission on Minnesota Resources (LCCMR). Additional support came from the Dow Chemical Company, Midland, MI. The Wind Power (2014) map was created by the National Renewable Energy Laboratory for the U.S. Department of Energy with data provided by AWS TruePower.

■ NOMENCLATURE

a = moles of ammonia produced (mol/h)
A = condenser interfacial area (m^2)
b, c = quadratic equation parameters
h_i = heat-transfer coefficient of component i
m = moles of gas mixture per hour in the recycle flow (mol/h)
k_1 = rate constant of the forward reaction
k_2 = rate constant of the reverse reaction
k_c = heat-transfer coefficient (mol/h·m^2)
k'_R = linearized catalytic reaction rate using eq 13 (mol/L·h)
k_R = linearized catalytic reaction rate using eq 1 (mol/L·h)
n_0 = total number of moles of gas present in the small-scale plant
P_i = partial pressure of component i
U = overall heat transfer
V_R = volume of catalyst (m^3)
X = fractional driving force in a normalized mole fraction scale
x_A^* = ammonia mole fraction at equilibrium
x_A^0 = mole fraction of ammonia at the condenser wall
x_i = mole fraction of component i in the recycle stream

Subscripts

A = ammonia
c = condenser
H = hydrogen
i = component i
j = internal
N = nitrogen
o = outer side
w = wall

Superscript

0 = phase equilibrium
* = equilibrium

Greek Letters

ΔH_{vap} = heat of vaporization (J/mol)
ΔT = temperature difference in the condenser

■ REFERENCES

(1) Stoltzenberg, D. *Fritz Haber: Chemist, Nobel Laureate, German, Jew*; Chemical Heritage Press: Philadelphia, 2004.
(2) Charles, D. *Master Mind: The Rise and Fall of Fritz Haber, the Nobel Laureate Who Launched the Age of Chemical Warfare*; Ecco: New York, 2005.
(3) *Energy Efficiency and CO_2 Emissions in Ammonia Production*; International Fertilizer Industry Association: Paris, France, 2009.
(4) Lan, R.; Irvine, J. T. S.; Tao, S. Ammonia and related chemicals as potential indirect hydrogen storage materials. *Int. J. Hydrogen Energy* **2012**, *37*, 1482.
(5) Patil, A.; Laumans, L.; Vrijenhoef, H. Solar to Ammonia – Via Proton's NFuel Units. *Procedia Eng.* **2014**, *83*, 322.
(6) Aguirre-Villegas, H. A.; Larson, R.; Reinemann, D. J. From waste-to-worth: Energy, emissions, and nutrient implications of manure processing pathways. *Biofuels, Bioprod. Biorefin.* **2014**, *8*, 770.
(7) Gilbert, P.; Alexander, S.; Thornley, P.; Brammer, J. Assessing economically viable carbon reductions for the production of ammonia from biomass gasification. *J. Cleaner Prod.* **2014**, *64*, 581.
(8) Bartels, J. R. A Feasibility Study of Implementing an Ammonia Economy. M.S. Thesis, Iowa State University, Ames, IA, 2008.
(9) Tunå, P.; Hulteberg, C.; Ahlgren, S. Techno-economic assessment of nonfossil ammonia production. *Environ. Prog. Sustainable Energy* **2013**, *33*, 1290.
(10) Tallaksen, J.; Bauer, F.; Hulteberg, C.; Reese, M.; Ahlgren, S. Nitrogen fertilizers manufactured using wind power: Greenhouse gas and energy balance of community-scale ammonia production. *J. Cleaner Prod.* **2015**, *107*, 626.
(11) Tiffany, D. G.; Reese, M.; Marquart, C. *Economic Evaluation of Deploying Small to Moderate Scale Ammonia Production Plants in Minnesota Using Wind and Grid-Based Electrical Energy Sources*; Minnesota Corn Research and Promotion Council: Shakopee, MN, 2015. http://tinyurl.com/ammonia-from-wind (Accessed February 3, 2015).
(12) Morgan, E.; Manwell, J.; McGowan, J. Wind-powered ammonia fuel production for remote islands: A case study. *Renewable Energy* **2014**, *72*, 51.
(13) Allman, W. A.; Daoutidis, P. Ammonia Supply Chains: A New Framework for Renewable Generation with a Case Study for Minnesota. To be presented at the *26th European Symposium on Computer Aided Process Engineering*, Portorož, Slovenia, Jun 12–15, 2016.
(14) National Renewable Energy Laboratory, (NREL) Wind Resource Map. 2014 - data provided by AWS TruePower. Available at http://www.nrel.gov/gis/wind.html. (Accessed September 17, 2015)
(15) Planted Corn Acreage by County. National Agricultural Statistics Service (NASS), Washington, DC, 2014.
(16) Kumar, A.; Daoutidis, P. Nonlinear dynamics and control of process systems with recycle. *J. Process Control* **2002**, *12*, 475.
(17) Baldea, M.; Daoutidis, P. *Dynamics and Nonlinear Control of Integrated Process Systems*; Cambridge University Press: Cambridge, U.K., 2012.
(18) Temkin, M. I.; Pyzhev, V. Kinetics of ammonia synthesis on promoted iron catalyst. *Acta Physiochim. USSR* **1940**, *12*, 327.
(19) Annable, D. Application of the Temkin kinetic equation to ammonia synthesis in large-scale reactors. *Chem. Eng. Sci.* **1952**, *1*, 145.
(20) Guacci, U.; Traina, F.; Ferraris, G. B.; Barisone, R. On the Application of the Temkin Equation in the Evaluation of Catalysts for the Ammonia Synthesis. *Ind. Eng. Chem. Process Des. Dev.* **1977**, *16*, 166.
(21) Jennings, J. R. *Catalytic Ammonia Synthesis: Fundamentals and Practice*; Plenum Press: New York, 1991.
(22) Cussler, E. L. *Diffusion: Mass Transfer in Fluid Systems*; Cambridge University Press: New York, 2009.
(23) Cavallini, A.; Censi, G.; Col, D. D.; Doretti, L.; Rossetto, L.; Longo, G. Heat Transfer Coefficients of HFC Refrigerants during Condensation at High Temperature Inside an Enhanced Tube. Presented at the *9th International Refrigeration Conference*; West Lafayette, IN, 2002; Paper 563.
(24) Green, D. W. Section 2: Physical and Chemical Data. In *Perry's Chemical Engineers' Handbook*; Perry, R. H., Green, D. W., Eds.; McGraw-Hill: New York, 2007.
(25) Geankoplis, C. J. *Transport Processes and Unit Operations*; PTR Prentice Hall: Engelwood Cliffs, NJ, 1993.

DOI: 10.1021/acs.iecr.5b04909
Ind. Eng. Chem. Res. 2016, 55, 3742–3750